**Wooseok Ji**
Research Fellow

**Anthony M. Waas**[1]
Felix Pawlowski Collegiate Professor
e-mail: dcw@umich.edu

Department of Aerospace Engineering,
Composite Structures Laboratory,
University of Michigan,
Ann Arbor, MI 48109

**Zdenek P. Bazant**
Walter Murphy Professor,
Department of Civil Engineering,
Northwestern University,
Evanston, IL 60208

# On the Importance of Work-Conjugacy and Objective Stress Rates in Finite Deformation Incremental Finite Element Analysis

*This paper is concerned with two issues that arise in the finite element analysis of 3D solids. The first issue examines the objectivity of various stress rates that are adopted in incremental analysis of solids. In doing so, it is revealed that large errors are incurred by an improper choice of stress rate. An example problem is presented to show the implications of the choice of stress rate. The second issue addresses the need to maintain work-conjugacy in formulating and solving bifurcation buckling problems of 3D elastic solids. Four popular commercial codes are used to obtain buckling loads of an axially compressed thick sandwich panel, and it is shown that large errors in buckling load predictions are incurred as a result of violating the requirement of work-conjugacy. Remedies to fix the errors in the numerical solution strategy are given.* [DOI: 10.1115/1.4007828]

## 1 Introduction

The finite element method is a key computational tool in solid mechanics, and it has now become the mainstay of problems involving any of the broad phenomena of material deformation—elasticity, plasticity, and damage. However, its utility for problems involving finite deformation of highly anisotropic materials, such as laminated composites, sandwich composites, and materials with distributed and aligned damage (sets of parallel microcracks), requires careful consideration in the definition and utility of various stresses and stress rates and associated work-conjugate strains and strain rates. In earlier work by Bazant [1], the requirements on the proper work definition that are necessary for the equivalence between different mathematical formulations for the incremental elastic stability of a 3D solid were presented. Among the various mathematical formulations available to address the infinitesimal elastic stability of a 3D solid, Bazant showed that, when a certain finite strain measure is selected to describe the incremental deformation, the corresponding conjugate incremental stress and the constitutive model associated with those choices of stress and strain must be used in order to properly define the internal work due to transitions in the equilibrium state. He also derived a unified general formulation in terms of a parameter $m$, with different values of $m$ leading to different mathematical formulations. His unified formulation provides consistency and correctness for obtaining the work-conjugate relations between the finite strain and the incremental stress and the corresponding constitutive model.

Modern commercial codes have formulated their finite element equations for certain classes of problems using stress rates. As is well known, the rate form of the resulting equations needs to be objective with respect to coordinate transformations. In this paper, it is shown that many popular commercial codes violate many of the tenets pointed out in Bazant [1] and later exemplified in Bazant and Cedolin [2] with respect to the proper use of objective stress rates and with respect to computing buckling loads of solids, leading to large discrepancies in computed outcomes. Simple remedies to fix these deficiencies are suggested. The implications of the reported findings are significant for structural analysts, since the errors pointed out are quite large for a range of problems that are of practical significance in structural design that use built-up structures or modern composite materials that exhibit strong anisotropy.

This paper is organized as follows: We first present various stress rates that are adopted in formulating incremental equations for analyzing nonlinear mechanics problems using the finite element method. This is followed by studying an example problem of shearing a block using four popular commercial codes. The results are compared against each other and an available analytical solution. Next, we consider the bifurcation buckling problems of a homogenized orthotropic strip and a thick orthotropic sandwich panel, analytically and within the context of using the finite element method to compute buckling loads. The results predicted by the commercial codes are compared against each other and the analytical solutions. The paper concludes with suggestions to fix the errors that are present in the commercial codes for the two types of problems discussed.

## 2 Basic Finite Element Formulation Using Objective Stress Rates

The equilibrium equation of a deformable solid can be written in a rate form using the nominal stress in the initial, reference state [3].

$$\nabla_{\mathbf{X}} \cdot \dot{\mathbf{N}} + \dot{\mathbf{b}} = \mathbf{0} \tag{1}$$

where $\nabla_{\mathbf{X}} \cdot \dot{\mathbf{N}}$ = divergence of $\dot{\mathbf{N}}$ with respect to the reference coordinate system, $\dot{\mathbf{N}}$ = rate of nominal stress change after an infinitesimal time, and $\dot{\mathbf{b}}$ = body force rate per unit volume of the

[1]Corresponding author.

Manuscript received April 1, 2012; final manuscript received July 22, 2012; accepted manuscript posted October 10, 2012; published online May 23, 2013. Editor: Yonggang Huang.

  

initial configuration. The corresponding traction boundary condition is

$$\dot{\mathbf{t}} = \mathbf{n} \cdot \dot{\mathbf{N}} \tag{2}$$

where $\dot{\mathbf{t}}$ = nominal traction rate prescribed on a surface in the initial state and $\mathbf{n}$ = unit normal of the surface in the reference configuration. The principle of virtual work with virtual velocity fields $\delta\mathbf{v}$ is employed to formulate the finite element equations corresponding to Eqs. (1) and (2). Integrating the scalar product between Eq. (1) and the virtual velocity fields over the volume in the reference configuration yields

$$\int_{V^B} \left(\nabla_{\mathbf{X}} \cdot \dot{\mathbf{N}} + \dot{\mathbf{b}}\right) \cdot \delta\mathbf{v}\, \mathrm{d}V^B = 0 \tag{3}$$

where $B$ represents quantities associated with the reference, base state. From the chain rule,

$$\int_{V^B} \left(\nabla_{\mathbf{X}} \cdot \left(\dot{\mathbf{N}} \cdot \delta\mathbf{v}\right) - \dot{\mathbf{N}} : \frac{\partial \delta\mathbf{v}}{\partial \mathbf{X}} + \dot{\mathbf{b}} \cdot \delta\mathbf{v}\right) \mathrm{d}V^B = 0 \tag{4}$$

Utilizing the Gauss theorem with the first term,

$$\int_{S^B} \mathbf{n} \cdot \dot{\mathbf{N}} \cdot \delta\mathbf{v}\, \mathrm{d}S^B + \int_{V^B} \left(-\dot{\mathbf{N}} : \frac{\partial \delta\mathbf{v}}{\partial \mathbf{X}} + \dot{\mathbf{b}} \cdot \delta\mathbf{v}\right) \mathrm{d}V^B = 0 \tag{5}$$

From Eq. (2), the final form of the virtual work equation is obtained as

$$\int_{V^B} \left(\dot{\mathbf{N}} : \frac{\partial \delta\mathbf{v}}{\partial \mathbf{X}}\right) \mathrm{d}V^B = \int_{S^B} \dot{\mathbf{t}} \cdot \delta\mathbf{v}\, \mathrm{d}S^B + \int_{V^B} \dot{\mathbf{b}} \cdot \delta\mathbf{v}\, \mathrm{d}V^B = 0 \tag{6}$$

Using the Kirchhoff stress, $\boldsymbol{\tau} = \mathbf{F} \cdot \mathbf{N}$, where $\mathbf{F}$ is the deformation gradient, the rate of nominal stress change is expressed as

$$\begin{aligned} \dot{\mathbf{N}} &= \mathbf{F}^{-1} \cdot \dot{\boldsymbol{\tau}} + \dot{\mathbf{F}}^{-1} \cdot \boldsymbol{\tau} \\ &= \mathbf{F}^{-1} \cdot \dot{\boldsymbol{\tau}} - \mathbf{F}^{-1} \cdot \mathbf{L} \cdot \boldsymbol{\tau} \end{aligned} \tag{7}$$

where $\mathbf{L} = \dot{\mathbf{F}} \cdot \mathbf{F}^{-1}$ = velocity gradient. Now, the internal virtual work rate, $\delta\dot{U}$, is expressed in terms of the rate of Kirchhoff stress, $\dot{\boldsymbol{\tau}}$, the velocity gradient, $\mathbf{L}$, and the virtual velocity gradient, $\delta\mathbf{L}$, such that

$$\begin{aligned} \delta\dot{U} &= \int_{V^B} \dot{N} : \frac{\partial \delta\mathbf{v}}{\partial \mathbf{X}} \mathrm{d}V^B \\ &= \int_{V_B} \left[\mathbf{F}^{-1} \cdot \left(\dot{\boldsymbol{\tau}} - \mathbf{L} \cdot \boldsymbol{\tau}\right)\right] : \frac{\partial \delta\mathbf{v}}{\partial \mathbf{X}} \mathrm{d}V^B \\ &= \int_{V^B} \mathrm{Tr}\left(\frac{\partial \delta\mathbf{v}}{\partial \mathbf{X}} \cdot \mathbf{F}^{-1} \cdot \left(\dot{\boldsymbol{\tau}} - \mathbf{L} \cdot \boldsymbol{\tau}\right)\right) \mathrm{d}V^B \\ &= \int_{V^B} \left(\dot{\boldsymbol{\tau}} - \boldsymbol{\tau} \cdot \mathbf{L}^T\right) : \delta\mathbf{L} \mathrm{d}V^B \end{aligned} \tag{8}$$

where Tr denotes the trace of a tensor. It is noted here that the symmetric property of the Kirchhoff stress is used in deriving Eq. (8). The rate of change of the Kirchhoff stress, $\dot{\boldsymbol{\tau}}$, in Eq. (8) can be expressed with various types of objective stress rates, which can be written in a unified form as

$$\overset{\nabla}{\boldsymbol{\tau}}{}^{(m)} = \overset{\nabla}{\boldsymbol{\tau}}{}^{(TK)} + \frac{1}{2}(2-m)(\mathbf{D} \cdot \boldsymbol{\tau} + \boldsymbol{\tau} \cdot \mathbf{D}) \tag{9}$$

where $\overset{\nabla}{\boldsymbol{\tau}}{}^{(TK)}$ is the objective Truesdell rate of Kirchhoff stress and $\mathbf{D}$ is the rate of deformation defined as $\mathbf{D} = \frac{1}{2}\left(\mathbf{L} + \mathbf{L}^T\right)$. The parameter "$m$" in Eq. (9) corresponds to different, specific types of objective rates of Kirchhoff stress. For example, $m = 2$ gives the objective Truesdell rate of Kirchhoff stress and $m = 0$ corresponds to the Jaumann rate. $\dot{\boldsymbol{\tau}}$ and $\overset{\nabla}{\boldsymbol{\tau}}{}^{(TK)}$ are connected through the definition of the objective Truesdell rate of Kirchhoff stress as

$$\overset{\nabla}{\boldsymbol{\tau}}{}^{(TK)} = \dot{\boldsymbol{\tau}} - \mathbf{L} \cdot \boldsymbol{\tau} - \boldsymbol{\tau} \cdot \mathbf{L}^T \tag{10}$$

The corresponding tangential moduli of $\overset{\nabla}{\boldsymbol{\tau}}{}^{(TK)}$ can be derived from the constitutive model associated with the second Piola–Kirchhoff stress, $\mathbf{S}$, and Green's Lagrangian strain, $\mathbf{E} = \frac{1}{2}(\mathbf{C} - \mathbf{I})$, where $\mathbf{C} = \mathbf{F}^T\mathbf{F}$ is the right Cauchy deformation tensor and $\mathbf{I}$ is the identity tensor of rank 2. When $U$ is the strain energy per unit initial volume of a solid, $\mathbf{S}$ can be obtained from

$$\mathbf{S} = \frac{\partial U}{\partial \mathbf{E}} \tag{11}$$

or in the form of a stress-strain relation,

$$\mathbf{S} = \mathbb{C} : \mathbf{E} \tag{12}$$

where $\mathbb{C}$ is the fourth order material elasticity tensor paired with the Green's Lagrangian strain defined as

$$\mathbb{C}_{IJKL} = \frac{\partial^2 U}{\partial E_{IJ} \partial E_{KL}} \tag{13}$$

The rate form of Eq. (12) is

$$\dot{\mathbf{S}} = \mathbb{C} : \dot{\mathbf{E}} \tag{14}$$

The Kirchhoff stress can be written in terms of the second Piola–Kirchhoff stress as

$$\boldsymbol{\tau} = \mathbf{F} \cdot \mathbf{S} \cdot \mathbf{F}^T \tag{15}$$

and the rate of change of the Kirchhoff stress is

$$\begin{aligned} \dot{\boldsymbol{\tau}} &= \dot{\mathbf{F}} \cdot \mathbf{S} \cdot \mathbf{F}^T + \mathbf{F} \cdot \mathbf{S} \cdot \dot{\mathbf{F}}^T + \mathbf{F} \cdot \dot{\mathbf{S}} \cdot \mathbf{F}^T \\ &= \mathbf{L} \cdot \boldsymbol{\tau} + \boldsymbol{\tau} \cdot \mathbf{L}^T + \mathbf{F} \cdot \left(\mathbb{C} : \dot{\mathbf{E}}\right) \cdot \mathbf{F}^T \end{aligned} \tag{16}$$

From the definition of the Truesdell rate in Eq. (10), Eq. (16) can be rearranged and rewritten in indicial notation as

$$\overset{\nabla(TK)}{\tau_{ij}} = F_{iI} F_{jJ} F_{kK} F_{lL} \mathbb{C}_{IJKL} D_{kl} \tag{17}$$

or

$$\overset{\nabla}{\boldsymbol{\tau}}{}^{(TK)} = \mathbb{C}^{(TK)} : \mathbf{D} \tag{18}$$

where $\mathbb{C}^{(TK)}_{ijkl} = F_{iI} F_{jJ} F_{kK} F_{lL} \mathbb{C}_{IJKL}$ is the spatial (or Eulerian) elasticity tensor. Now, Eq. (9) is expressed as

$$\overset{\nabla}{\boldsymbol{\tau}}{}^{(m)} = \mathbb{C}^{(TK)} : \mathbf{D} + \frac{1}{2}(2-m)(\mathbf{D} \cdot \boldsymbol{\tau} + \boldsymbol{\tau} \cdot \mathbf{D}) \tag{19}$$

or, utilizing $\delta_{ij}$ (identity tensor of rank 2), it can be written in indicial notation as

$$\begin{aligned} \overset{\nabla(m)}{\tau_{ij}} &= \left[\mathbb{C}^{(TK)}_{ijkl} + \frac{1}{2}(2-m)\left\{\tau_{ik}\delta_{jl} + \tau_{jl}\delta_{ik}\right\}\right] D_{kl} \\ &= \left[\mathbb{C}^{(TK)}_{ijkl} + \frac{1}{4}(2-m)\left(\tau_{ik}\delta_{jl} + \tau_{jk}\delta_{il} + \tau_{il}\delta_{jk} + \tau_{jl}\delta_{ik}\right)\right] D_{kl} \end{aligned} \tag{20}$$

with addition of the minor symmetry property of the fourth order tensor. Hence, the unified objective stress rate is written in the form of elasticity as

$$\overset{\nabla}{\boldsymbol{\tau}}{}^{(m)} = \mathbb{C}^{(m)} : \mathbf{D} \tag{21}$$

where

$$\mathbb{C}^{(m)}_{ijkl} = \mathbb{C}^{(TK)}_{ijkl} + \frac{1}{4}(2-m)\left(\tau_{ik}\delta_{jl} + \tau_{jk}\delta_{il} + \tau_{il}\delta_{jk} + \tau_{jl}\delta_{ik}\right) \tag{22}$$

From Eqs. (9), (10), and Eq. (21), Eq. (8) is rewritten as

$$\begin{aligned}\delta\dot{U} &= \int_{V^B}\left[\overset{\nabla}{\boldsymbol{\tau}}{}^{(m)} - \frac{1}{2}(2-m)(\mathbf{D}\cdot\boldsymbol{\tau} + \boldsymbol{\tau}\cdot\mathbf{D}) + L\cdot\boldsymbol{\tau}\right] : \delta\mathbf{L}\,dV^B \\ &= \int_{V^B}\left[\overset{\nabla}{\boldsymbol{\tau}}{}^{(m)} : \delta\mathbf{D} - (2-m)\boldsymbol{\tau} : (\mathbf{D}\cdot\delta\mathbf{D}) + \boldsymbol{\tau} : \left(\mathbf{L}^T\cdot\delta\mathbf{L}\right)\right]dV^B\end{aligned} \tag{23}$$

Thus, the principle of virtual work in the reference configuration is written as

$$\begin{aligned}&\int_{V^B}\left[\overset{\nabla}{\boldsymbol{\tau}}{}^{(m)} : \delta\mathbf{D} - (2-m)\boldsymbol{\tau} : (\mathbf{D}\cdot\delta\mathbf{D}) + \tau : \left(\mathbf{L}^T\cdot\delta\mathbf{L}\right)\right]dV^B \\ &\quad = \int_{S^B}\dot{\mathbf{t}}\cdot\delta\mathbf{v}\,dS^B + \int_{V^B}\dot{\mathbf{b}}\cdot\delta\mathbf{v}\,dV^B = 0\end{aligned} \tag{24}$$

or, in the current (deformed) configuration, it reads

$$\begin{aligned}&\int_{V}\left[\overset{\nabla}{\boldsymbol{\sigma}}{}^{(m)} : \delta\mathbf{D} - (2-m)\boldsymbol{\sigma} : (\mathbf{D}\cdot\delta\mathbf{D}) + \boldsymbol{\sigma} : \left(\mathbf{L}^T\cdot\delta\mathbf{L}\right)\right]dV \\ &\quad = \int_{S}\dot{\mathbf{t}}'\cdot\delta\mathbf{v}dS + \int_{V}\dot{\mathbf{b}}'\cdot\delta\mathbf{v}\,dV = 0\end{aligned} \tag{25}$$

where $\overset{\nabla}{\boldsymbol{\sigma}}{}^{(m)} = J^{-1}\overset{\nabla}{\boldsymbol{\tau}}{}^{(m)}$ and $\boldsymbol{\sigma}$ is the Cauchy stress that is related to the Kirchhoff stress through

$$\boldsymbol{\tau} = J\boldsymbol{\sigma} \tag{26}$$

where $J = dV/dV^B$ is the determinant of the deformation gradient. We now conclusively provide the basis of the rate-based finite element formulation. This formulation consists of Eq. (21) for stress increments, Eq. (22) for the corresponding constitutive model, and Eqs. (24) or (25) for the equilibrium statement in the initial or current deformed configuration, respectively. The following sections (Secs. 2.1–2.6) discuss the different formulations that employ different stress rates depending on the parameter "$m$". It is noted here that, when stresses are being updated in finite element analysis, it is crucial to maintain a consistent formulation between Eq. (21) and Eq. (22) if the principle of virtual work is correctly implemented using any choice of stress rate. The choice of different stress rate types is solely dependent on the efficiency of solving a particular type of problem. Depending on the value of "$m$", the resulting mathematical expressions may be different, but they are mutually equivalent to each other, providing the same end result.

**2.1 Formulation A: Truesdell Rate of Kirchhoff Stress.** The formulation based on the objective Truesdell rate of Kirchhoff stress is obtained when $m = 2$. From Eq. (9), $\overset{\nabla}{\boldsymbol{\tau}}{}^{(2)} = \overset{\nabla}{\boldsymbol{\tau}}{}^{(TK)}$. The principle of virtual work in the initial configuration, Eq. (24), is written as

$$\int_{V^B}\overset{\nabla}{\boldsymbol{\tau}}{}^{(TK)} : \delta\mathbf{D} + \boldsymbol{\tau} : \left(\mathbf{L}^T\cdot\delta\mathbf{L}\right)dV^B = \int_{S^B}\dot{\mathbf{t}}\cdot\delta\mathbf{v}\,dS^B + \int_{V^B}\dot{\mathbf{b}}\cdot\delta\mathbf{v}\,dV^B \tag{27}$$

and the corresponding spatial elasticity tensor is $\mathbb{C}^{(2)}_{ijkl} = \mathbb{C}^{(TK)}_{ijkl} = F_{iI}F_{jJ}F_{kK}F_{lL}\mathbb{C}_{IJKL}$. In many practical cases, the internal work needs to be second order accurate to describe the equilibrium state of a solid after infinitesimal increments, as shown in Ref. [2] (see Chapter 11.3). In this case, higher order terms in Eq. (18) can be neglected and the tangential moduli are simplified to the infinitesimal form of

$$\mathbb{C}^{(2)}_{ijkl} \simeq \delta_{iI}\delta_{jJ}\delta_{kK}\delta_{lL}\mathbb{C}_{IJKL} = \mathbb{C}_{ijkl} \tag{28}$$

**2.2 Formulation B: Truesdell Rate of Cauchy Stress.** Next, the Truesdell rate of Cauchy stress is utilized to express the principle of virtual work in the current deformed configuration. With $m = 2$, Eq. (25) is written as

$$\int_{V}\left[\overset{\nabla}{\boldsymbol{\sigma}}{}^{(2)} : \delta\mathbf{D} + \boldsymbol{\sigma} : \left(\mathbf{L}^T\cdot\delta\mathbf{L}\right)\right]dV = \int_{S}\dot{\mathbf{t}}'\cdot\delta\mathbf{v}\,dS + \int_{V}\dot{\mathbf{b}}'\cdot\delta\mathbf{v}\,dV \tag{29}$$

The Truesdell rate of Cauchy stress is defined as

$$\overset{\nabla}{\boldsymbol{\sigma}}{}^{(2)} = \overset{\nabla}{\boldsymbol{\sigma}}{}^{(TC)} = \dot{\boldsymbol{\sigma}} - \mathbf{L}\cdot\boldsymbol{\sigma} - \boldsymbol{\sigma}\cdot\mathbf{L}^T + \mathrm{Tr}(\mathbf{L})\boldsymbol{\sigma} \tag{30}$$

and it can be written in terms of the Truesdell rate of Kirchhoff stress as

$$\overset{\nabla}{\boldsymbol{\sigma}}{}^{(TC)} = J^{-1}\overset{\nabla}{\boldsymbol{\tau}}{}^{(TC)} \tag{31}$$

Thus, the spatial elasticity tensor for $\overset{\nabla}{\boldsymbol{\sigma}}{}^{(TC)}$ is obtained as $\mathbb{C}^{(TC)} = J^{-1}\mathbb{C}^{(TK)}$. However, when we impose the same assumption on the need for second order accurate internal work due to stress increments, the Truesdell rate of Cauchy stress can be directly derived from the simplification of the Truesdell rate of Kirchhoff stress, such that

$$\begin{aligned}\overset{\nabla}{\boldsymbol{\tau}}{}^{(TK)} &= (\dot{J}\boldsymbol{\sigma}) - \mathbf{L}\cdot(J\boldsymbol{\sigma}) - (J\boldsymbol{\sigma})\cdot\mathbf{L}^T \\ &\simeq \dot{\boldsymbol{\sigma}} + \mathrm{Tr}(\mathbf{L})\boldsymbol{\sigma} - \mathbf{L}\cdot\boldsymbol{\sigma} - \boldsymbol{\sigma}\cdot\mathbf{L}^T \\ &= \overset{\nabla}{\boldsymbol{\sigma}}{}^{(TC)}\end{aligned} \tag{32}$$

where the Jacobian is approximated as $J \simeq 1 + u_{k,k}$ and $\left(\dot{J\sigma_{ij}}\right) = J\dot{\sigma}_{ij} + \dot{J}\sigma_{ij} \simeq \dot{\sigma}_{ij} + v_{k,k}\sigma_{ij}$. Higher order terms associated with $u_{k,k}$ are neglected in deriving Eq. (32), since they are not important in defining incremental internal work to second order accuracy. Therefore, the elasticity tensor for $\overset{\nabla}{\boldsymbol{\sigma}}{}^{(TC)}$ is obtained as $\mathbb{C}^{(TC)} = \mathbb{C}$, where the internal work is preserved to second order accuracy.

**2.3 Formulation C: Jaumann Rate of Kirchhoff Stress.** The Jaumann rate is a popular choice in modern computational continuum mechanics, because it is relatively easy to implement into a finite element framework (for example, the spin tensor $\mathbf{W}$ is readily available as a by-product of $\mathbf{D}$) and leads to symmetric tangential moduli. The Jaumann rate of Kirchhoff stress is defined as

$$\overset{\nabla}{\boldsymbol{\tau}}{}^{(0)} = \overset{\nabla}{\boldsymbol{\tau}}{}^{(JK)} = \dot{\boldsymbol{\tau}} + \boldsymbol{\tau}\cdot\mathbf{W} - \mathbf{W}\cdot\boldsymbol{\tau} \tag{33}$$

Substitution of $m = 0$ into Eq. (24) yields the principle of virtual work based on the Jaumann rate of Kirchhoff stress,

$$\begin{aligned}&\int_{V^B}\left[\overset{\nabla}{\boldsymbol{\tau}}{}^{(0)} : \delta\mathbf{D} - 2\boldsymbol{\tau} : (\mathbf{D}\cdot\delta\mathbf{D}) + \boldsymbol{\tau} : \left(\mathbf{L}^T\cdot\delta\mathbf{L}\right)\right]dV^B \\ &\quad = \int_{S^B}\dot{\mathbf{t}}\cdot\delta\mathbf{v}dS^B + \int_{V^B}\dot{\mathbf{b}}\cdot\delta\mathbf{v}\,dV^B\end{aligned} \tag{34}$$

and the corresponding tangential moduli are

$$\mathbb{C}^{(0)}_{ijkl} = \mathbb{C}^{(JK)}_{ijkl} = \mathbb{C}^{(TK)}_{ijkl} + \frac{1}{2}\left(\tau_{ik}\delta_{jl} + \boldsymbol{\tau}_{jk}\delta_{il} + \boldsymbol{\tau}_{il}\delta_{jk} + \boldsymbol{\tau}_{jl}\delta_{ik}\right) \quad (35)$$

When we define the second order accurate internal work, only the first order terms in the constitutive model in Eq. (35) are required [2]. Since the Jacobian can be approximated as $J = 1 + u_{k,k}$, Eq. (35) is now reduced to

$$\mathbb{C}^{(0)}_{ijkl} = \mathbb{C}_{ijkl} + \frac{1}{2}\left(\sigma_{ik}\delta_{jl} + \sigma_{jk}\delta_{il} + \sigma_{il}\delta_{jk} + \sigma_{jl}\delta_{ik}\right) \quad (36)$$

**2.4 Formulation D: Biezeno–Hencky Rate of Cauchy Stress.** The principle of virtual work in terms of the objective Biezeno–Hencky rate of Cauchy stress can be obtained from Eq. (25) with $m = 0$,

$$\int_V \left[\overset{\nabla}{\boldsymbol{\sigma}}{}^{(0)} : \delta\mathbf{D} - 2\boldsymbol{\sigma} : (\mathbf{D}\cdot\delta\mathbf{D}) + \boldsymbol{\sigma} : \left(\mathbf{L}^T\cdot\delta\mathbf{L}\right)\right] dV = \int_S \dot{\mathbf{t}}'\cdot\delta\mathbf{v}\, dS + \int_V \dot{\mathbf{b}}'\cdot\delta\mathbf{v}\, dV \quad (37)$$

The objective Biezeno–Hencky rate of Cauchy stress is defined as

$$\overset{\nabla}{\boldsymbol{\sigma}}{}^{(0)} = \overset{\nabla}{\boldsymbol{\sigma}}{}^{(BC)} = \dot{\boldsymbol{\sigma}} + \boldsymbol{\sigma}\cdot\mathbf{W} - \mathbf{W}\cdot\boldsymbol{\sigma} + \mathrm{Tr}(\mathbf{L})\boldsymbol{\sigma} \quad (38)$$

and it is related to the Jaumann rate of Kirchhoff stress through

$$\overset{\nabla}{\boldsymbol{\sigma}}{}^{(BC)} = J^{-1}\overset{\nabla}{\boldsymbol{\tau}}{}^{(JK)} \quad (39)$$

Thus, the material tensor for the Biezeno–Hencky stress rate of Cauchy stress is expressed as

$$\mathbb{C}^{(BC)}_{ijkl} = J^{-1}\mathbb{C}^{(TK)}_{ijkl} + \frac{1}{2}\left(\sigma_{ik}\delta_{jl} + \sigma_{jk}\delta_{il} + \sigma_{il}\delta_{jk} + \sigma_{jl}\delta_{ik}\right) \quad (40)$$

Again, when we define the internal work of stress increments to preserve second order accuracy, the Jaumann rate of Kirchhoff stress is simplified to

$$\begin{aligned}\overset{\nabla}{\boldsymbol{\tau}}{}^{(JK)} &= (\dot{J}\boldsymbol{\sigma}) + (J\boldsymbol{\sigma})\cdot\mathbf{W} - \mathbf{W}\cdot(J\boldsymbol{\sigma}) \\ &\simeq \dot{\boldsymbol{\sigma}} + \mathrm{Tr}(\mathbf{L})\boldsymbol{\sigma} + \boldsymbol{\sigma}\cdot\mathbf{W} - \mathbf{W}\cdot\boldsymbol{\sigma} \\ &= \overset{\nabla}{\boldsymbol{\sigma}}{}^{(BC)}\end{aligned} \quad (41)$$

and thus the material tensor for the Biezeno–Hencky stress rate of Cauchy stress is expressed as

$$\mathbb{C}^{(BC)}_{ijkl} = \mathbb{C}_{ijkl} + \frac{1}{2}\left(\sigma_{ik}\delta_{jl} + \sigma_{jk}\delta_{il} + \sigma_{il}\delta_{jk} + \sigma_{jl}\delta_{ik}\right) \quad (42)$$

**2.5 Formulation E: Jaumann Rate of Cauchy Stress.** The Jaumann rate of Cauchy stress can be regarded as a special case of the Biezeno–Hencky formulation where the term associated with the volumetric deformation, $\mathrm{Tr}(\mathbf{L})\sigma$, in Eq. (38) is neglected. The Jaumann rate of Cauchy stress is defined as

$$\overset{\nabla}{\boldsymbol{\sigma}}{}^{(JC)} = \dot{\boldsymbol{\sigma}} + \boldsymbol{\sigma}\cdot\mathbf{W} - \mathbf{W}\cdot\boldsymbol{\sigma} \quad (43)$$

Following steps similar to those adopted so far, the principle of virtual work in the current deformed configuration can be expressed in terms of $\overset{\nabla}{\boldsymbol{\sigma}}{}^{(JC)}$ and $\boldsymbol{\sigma}$, and it reads

$$\int_V \left[\overset{\nabla}{\boldsymbol{\sigma}}{}^{(JC)} : \delta\mathbf{D} - 2\boldsymbol{\sigma} : (\mathbf{D}\cdot\delta\mathbf{D}) + \boldsymbol{\sigma} : \left(\mathbf{L}^T\cdot\delta\mathbf{L}\right) + \mathrm{Tr}(\mathbf{L})\boldsymbol{\sigma} : \delta\mathbf{D}\right] dV = \int_S \dot{\mathbf{t}}'\cdot\delta\mathbf{v}\, dS + \int_V \dot{\mathbf{b}}'\cdot\delta\mathbf{v}\, dV \quad (44)$$

Bazant [1] showed that the Jaumann rate of Cauchy stress is not energetically conjugate to any strain measure. Ji et al. [4] demonstrated that a significant error is induced in computing buckling loads if a constant material tensor is used with the Jaumann rate of Cauchy stress. The deficiency of the Jaumann rate of Cauchy stress can be corrected by redefining the elasticity tensor as

$$\mathbb{C}^{(JC)}_{ijkl} = \mathbb{C}^{(BC)}_{ijkl} - \sigma_{ij}\delta_{kl} \quad (45)$$

as shown in page 727 of Ref. [2], where it is given as Eq. 11.4.6. Equation (45) converts Eqs. (44) to (37). The use of this transformation in an incremental analysis to extract buckling loads, for example, is described in Ref. [5].

**2.6 Summary of Formulations.** The principle of virtual work expressed using various types of stress rates are summarized here with the corresponding elasticity tensors in the infinitesimal form based on defining internal work to second order accuracy. It should be noted that the different formulations described in this presentation result in the same internal virtual work rate defined in Eq. (8). The end result of a boundary value problem solution will be the same, regardless of the type of objective stress rate used in carrying out the solution.

- Formulation A: Truesdell rate of Kirchhoff stress

$$\int_{V^B} \overset{\nabla}{\boldsymbol{\tau}}{}^{(TK)} : \delta\mathbf{D} + \boldsymbol{\tau} : \left(\mathbf{L}^T\cdot\delta\mathbf{L}\right) dV^B = \int_{S^B} \dot{\mathbf{t}}\cdot\delta\mathbf{v}\, dS^B + \int_{V^B} \dot{\mathbf{b}}\cdot\delta\mathbf{v}\, dV^B \quad (46a)$$

$$\mathbb{C}^{(TK)} = \mathbb{C} \quad (46b)$$

- Formulation B: Truesdell rate of Cauchy stress

$$\int_V \left[\overset{\nabla}{\boldsymbol{\sigma}}{}^{(TC)} : \delta\mathbf{D} + \boldsymbol{\sigma} : \left(\mathbf{L}^T\cdot\delta\mathbf{L}\right)\right] dV = \int_S \dot{\mathbf{t}}'\cdot\delta\mathbf{v}\, dS + \int_V \dot{\mathbf{b}}'\cdot\delta\mathbf{v}\, dV \quad (47a)$$

$$\mathbb{C}^{(TC)} = \mathbb{C} \quad (47b)$$

- Formulation C: Jaumann rate of Kirchhoff stress

$$\int_{V^B} \left[\overset{\nabla}{\boldsymbol{\tau}}{}^{(JK)} : \delta\mathbf{D} - 2\boldsymbol{\tau} : (\mathbf{D}\cdot\delta\mathbf{D}) + \boldsymbol{\tau} : \left(\mathbf{L}^T\cdot\delta\mathbf{L}\right)\right] dV^B = \int_S \dot{\mathbf{t}}\cdot\delta\mathbf{v}\, dS^B + \int_V \dot{\mathbf{b}}\cdot\delta\mathbf{v}\, dV^B \quad (48a)$$

$$\mathbb{C}^{(JK)}_{ijkl} = \mathbb{C}_{ijkl} + \frac{1}{2}\left(\sigma_{ik}\delta_{jl} + \sigma_{jk}\delta_{il} + \sigma_{il}\delta_{jk} + \sigma_{jl}\delta_{ik}\right) \quad (48b)$$

- Formulation D: Biezeno–Hencky rate of Cauchy stress

$$\int_V \left[\overset{\nabla}{\boldsymbol{\sigma}}{}^{(BC)} : \delta\mathbf{D} - 2\boldsymbol{\sigma} : (\mathbf{D}\cdot\delta\mathbf{D}) + \boldsymbol{\sigma} : \left(\mathbf{L}^T\cdot\delta\mathbf{L}\right)\right] dV = \int_S \dot{\mathbf{t}}'\cdot\delta\mathbf{v}\, dS + \int_V \dot{\mathbf{b}}'\cdot\delta\mathbf{v}\, dV \quad (49a)$$

$$\mathbb{C}^{(BC)}_{ijkl} = \mathbb{C}_{ijkl} + \frac{1}{2}\left(\sigma_{ik}\delta_{jl} + \sigma_{jk}\delta_{il} + \sigma_{il}\delta_{jk} + \sigma_{jl}\delta_{ik}\right) \quad (49b)$$

- Formulation E: Jaumann rate of Cauchy stress

$$\int_V \left[\overset{\nabla}{\boldsymbol{\sigma}}{}^{(JC)} : \delta\mathbf{D} - 2\boldsymbol{\sigma} : (\mathbf{D}\cdot\delta\mathbf{D}) + \boldsymbol{\sigma} : \left(\mathbf{L}^T\cdot\delta\mathbf{L}\right) + \mathrm{Tr}(\mathbf{L})\boldsymbol{\sigma} : \delta\mathbf{D}\right] dV = \int_S \dot{\mathbf{t}}'\cdot\delta\mathbf{v}\, dS + \int_V \dot{\mathbf{b}}'\cdot\delta\mathbf{v}\, dV \quad (50a)$$

$$\mathbb{C}^{(JC)}_{ijkl} = \mathbb{C}_{ijkl} - \sigma_{ij}\delta_{kl} + \frac{1}{2}\left(\sigma_{ik}\delta_{jl} + \sigma_{jk}\delta_{il} + \sigma_{il}\delta_{jk} + \sigma_{jl}\delta_{ik}\right) \quad (50b)$$

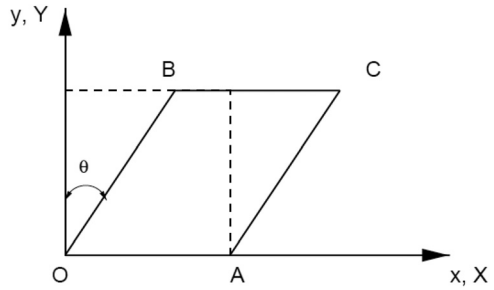


**Fig. 1 Configuration of the simple shear test problem**

## 3 Finite Element Analysis Demonstrating Incorrect Formulation

First, we will demonstrate the effect of using an incorrect formulation, resulting in incorrect tangential moduli (Eq. (22)). As discussed in Sec. 2, when an objective stress rate is used with the associated constitutive material model, the internal virtual work is correctly defined. Here, the formulation using the Jaumann rate of Cauchy stress with *constant moduli* is employed to demonstrate errors caused by the incorrect internal work definition. The Jaumann stress rate is chosen because many commercial finite element analysis (FEA) software packages utilize the Jaumann rate in their FE formulations. The formulation using the Jaumann stress rate of the Cauchy stress with constant moduli is denoted as "Formulation F", and the resulting solutions using Formulation F are compared against an analytical solution and the correct FEA solution. The commercial code ABAQUS is employed here to demonstrate errors caused by the incorrect definition of the internal virtual work. ABAQUS uses the Jaumann rate and defines the exact consistent Jacobian as

$$\tilde{\mathbb{C}} = \frac{1}{J}\frac{\partial \Delta(J\sigma)}{\partial \Delta\varepsilon} \tag{51}$$

where $\Delta\varepsilon$ = logarithmic strain increment. Formulation F is implemented through a user subroutine to show that it corresponds to the incorrect internal virtual work definition as used in the built-in ABAQUS procedure.

The simple shear test proposed by Dienes [6] is used as the boundary value problem. It is known that the Jaumann rate of Cauchy stress exhibits shear stress oscillations [6,7]. Thus, this example will be used to identify the type of objective stress rate used in ABAQUS and also to demonstrate the effect of using the incorrect tangential moduli in the formulation. The incorrect tangential moduli also lead to errors in updating the stress in an incremental analysis. The initially square plate, OACB, is subjected to simple shear, as illustrated in Fig. 1. Initially, only one plane strain element is used to avoid any interaction between elements. The bottom horizontal surface is restricted from moving in the $x$ and $y$ directions, and the top surface, CB, is constrained from moving in the $y$ direction. The top surface CB is subjected to a fixed displacement in the x direction.

Figure 2 shows the shear response predicted using various commercial FE codes as well as the correct theoretical solution, which uses the Truesdell rate. Analytical solutions using Green–Naghdi and Jaumann stress rates implemented with constant moduli are also plotted in Fig. 2. The theoretical solutions for the simple shear problem are available in Ref. [8]. Nonlinear static solvers are used from each FE program with the effect of the large strain deformation accounted for. It appears that NASTRAN is based on the Truesdell stress rate, and its output is in agreement with the correct analytical solution. The ANSYS code is based on the Green–Naghdi stress rate formulation, as shown in Fig. 2. LS-Dyna produces an oscillatory shear response, implying that its nonlinear static solver is based on the Jaumann stress rate formulation. Furthermore, it is confirmed that the ABAQUS built-in

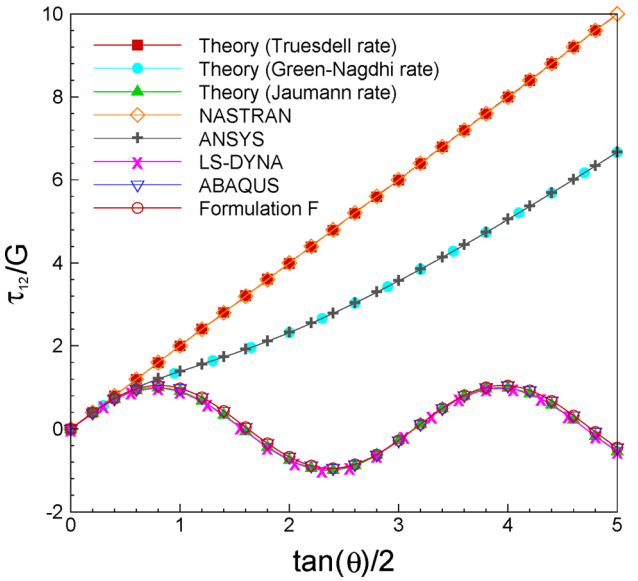


**Fig. 2 Numerical and theoretical solutions of the simple shear problem from different types of objectivity stress rates with constant tangential moduli**

formulation, which is based on the Jaumann rate of the Cauchy stress, corresponds to Formulation F, where the material elasticity tensor is assumed to be constant (which is incorrect). Here, formulation F is implemented in ABAQUS through a user subroutine. In the analytical solution based on the Jaumann rate, *constant* tangential moduli have been used. Furthermore, there is no "correct" theoretical solution that can employ the Jaumann rate, because it is not energetically work-conjugate to any strain measure, as pointed out in Ref. [2], except in certain classes of problems where incompressibility can be used as an additional assumption. On the other hand, the Truesdell rate with the correct tangential moduli (which are constant) does indeed provide the expected shear response.

When more than one element is used for the simple shear problem, proper traction boundary conditions must be prescribed on the lateral, vertical edges to maintain the deformation gradient for the simple shear over the entire body [9]. Alternatively, with periodic boundary conditions applied on the lateral surfaces (surface OB and AC in Fig. 1), the representative shear stress can be obtained from the element at the center, regardless of the number of elements used. Figure 3 shows the shear response of a rectangular strip when the horizontal length of the undeformed block is 10 times longer than the undeformed vertical length. Clearly, for the multiple element cases, all the erroneous formulations do provide the same consistent, nonphysical result as in the one element case, establishing that the error incurred is not dependent on mesh effects or size effects. Although results from ABAQUS are used here to discuss the effect of the boundary conditions on the edges, other FE codes show the same behavior, but those results are omitted for the sake of brevity.

## 4 Bifurcation Buckling Computations of Thick Orthotropic Structures—Comparisons Between Popular Commercial Codes

**4.1 Buckling Load Prediction for an Orthotropic Strip.** Ji et al. [4] demonstrated errors caused by the improper and incorrect formulations in a homogeneous, 2D orthotropic strip-buckling analysis. They showed that errors in predicting buckling load are as large as 100% when constant tangential moduli are used with the Jaumann rate of Cauchy stress. The effect of the incorrect formulation in using the constant moduli together with the Jaumann

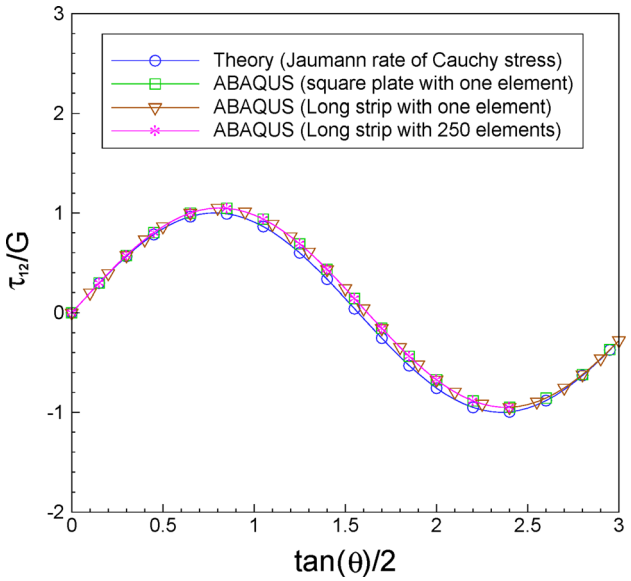


**Fig. 3 Shear stress obtained from a long strip FE model using periodic boundary conditions**

rate of the Cauchy stress has been ignored in the FEA community. The stress rate-based FEA has been extensively developed and utilized for characterizing the mechanical behavior of elastoplastic-type materials, whose elastic deformation part is usually assumed to be small compared to the plastic deformation. Consequently, since the problem then becomes dominated by the assumption of incompressibility invoked in standard plasticity formulations, the error caused by using the incorrect stress rate becomes masked. However, when an orthotropic elastic material is considered in a buckling problem, the incorrect formulation does lead to a significant overprediction in computing a buckling load [4]. Ji et al. showed that, when the FE formulation for a buckling problem fails to account for the correct pairing relations between stress, strain, and tangential moduli, errors in predicting the buckling load could be as large as 100%. The missing volumetric term pointed out in Ref. [4] results in a significant error because the orthotropic material exhibits directional-dependent deformation. They found that the popular commercial package, ABAQUS, overpredicts the buckling loads. Here, other popular commercial codes are also examined for the same buckling problem that was considered in Ref. [4]. Buckling loads computed from ANSYS, NASTRAN, and LS-Dyna are compared with those from the correct work-conjugate FE formulation [4] as well as analytical solutions based on elasticity theory [10].

The elastic and homogeneous orthotropic strip, as shown in Fig. 4, is uniformly compressed from one end, while the other end is restrained from axial deformation. The right edge remains straight but is free to move in the y-direction. Buckling behavior of the orthotropic strip is examined for two cases: first when the aspect ratio between the length and height of the strip varies and second when the ratio between the longitudinal and transverse direction stiffness changes. Material properties for the two cases are

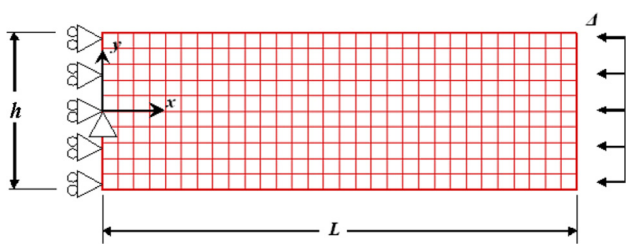


**Fig. 4 Orthotropic strip under uniform axial compression**

**Table 1 Material properties of a orthotropic strip for Case 1**

| Property | Value |
|---|---|
| $E_{xx}$(GPa) | $2000 \times G_{xy}$ |
| $E_{yy}$(GPa) | $2 \times G_{xy}$ |
| $G_{xy}$(GPa) | 7.17 |
| $\nu_{xy}$ | 0.29 |
| h (m) | 1 |
| L/h | $1 \sim 9$ |

**Table 2 Material properties of a orthotropic strip for Case 2**

| Property | Value |
|---|---|
| $E_{xx}$(GPa) | $1 \sim 1000 \times E_{yy}$ |
| $E_{yy}$(GPa) | $2 \times G_{xy}$ |
| $G_{xy}$(GPa) | 7.17 |
| $\nu_{xy}$ | 0.29 |
| h (m) | 1 |
| L/h | 3 |

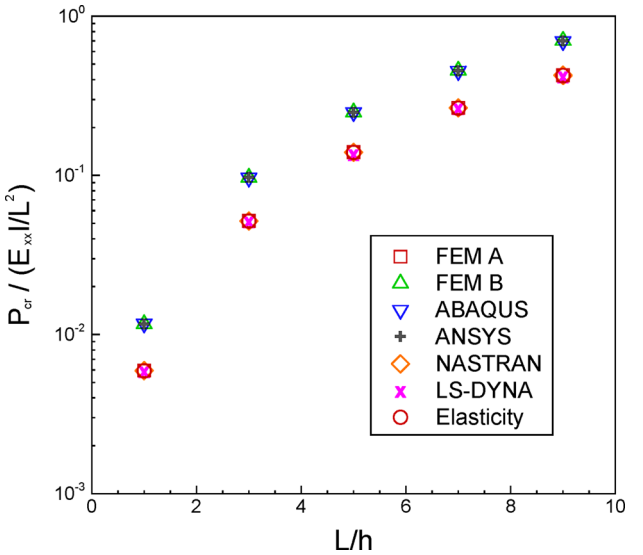


**Fig. 5 Buckling load predictions from various commercial FEA programs as a function of the aspect ratio**

summarized in Table 1 and Table 2, respectively. In both cases, the out-of-plane properties are $E_{zz} = E_{yy}$, $G_{xz} = G_{xy}$, $G_{yz} = 5.96$ GPa, $\nu_{xz} = 0.0159$, and $\nu_{yz} = 0.49$.

Figure 5 shows the buckling load predictions from various FEA programs, as the aspect ratio of the strip is varied. The orthotropic strip is assumed to be deformed in a plane strain setting, and linear quadrilateral plane strain elements are used for the buckling FE analyses. FEM A and FEM B are the finite element programs that are based on the study by Ji et al. [4]. FEM A denotes the finite element method based on the $m = 2$ formulation and FEM B is based on the $m = 0$ formulation, but used with the constant tangential moduli incorrectly. In FEM B, the constant tangential moduli (that should be paired with the $m = 2$ formulation) are intentionally used to demonstrate the effect of the improper use of the nonwork conjugate pairs. Various commercial FEA packages are also used to compute the buckling loads of the orthotropic strip, whose results are shown in Fig. 5. *BUCKLE and CPE4 elements are used in the ABAQUS 6.11 version. In other codes, for the buckling analysis, ANTYPE 1 of ANSYS 13.0 is employed with static analysis to obtain the prebuckling stress state of the

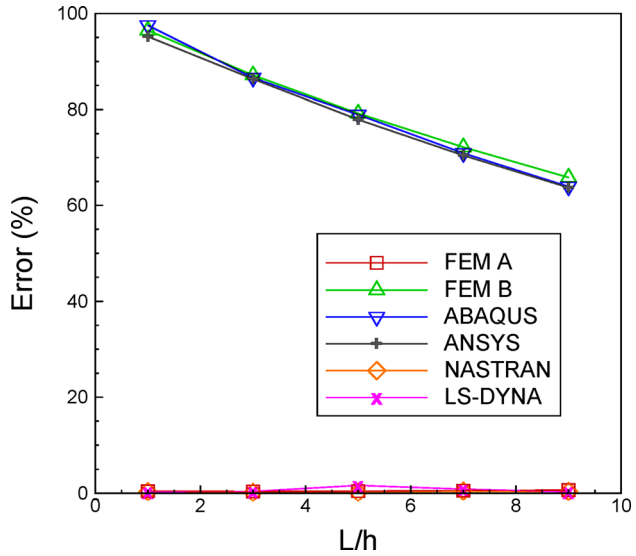


**Fig. 6 Errors in predicting buckling loads shown in Fig. 5**

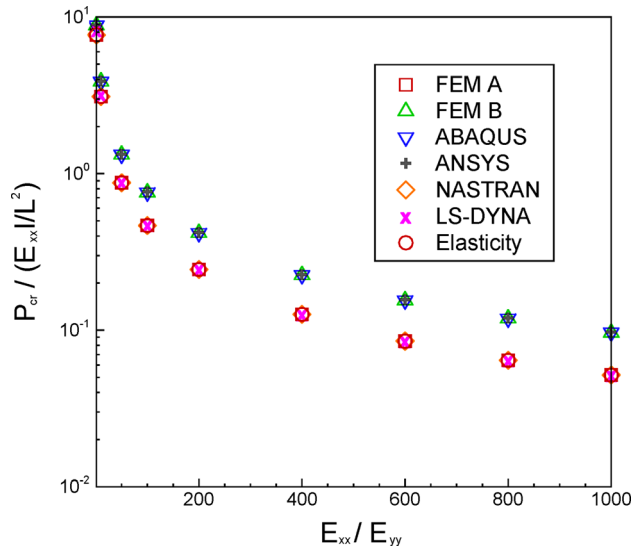


**Fig. 7 Buckling load predictions from various commercial FEA programs as a function of the stiffness ratio between the longitudinal and transverse direction**

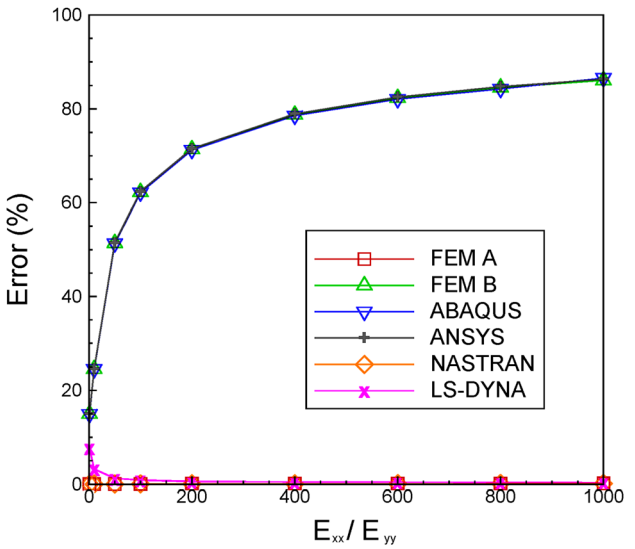


**Fig. 8 Errors in predicting buckling loads for a thick orthotropic strip shown in Fig. 7**

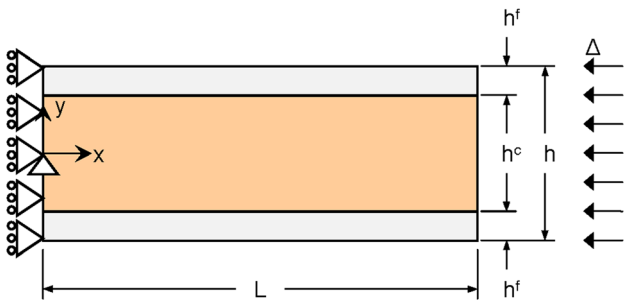


**Fig. 9 Configuration of an axially compressed sandwich panel**

strip. SOL 600 SEBUCKLE of NASTRAN 2011 with the Marc solver is utilized to account for the orthotropic material properties in a plane strain deformation. LS-Dyna also provides bifurcation buckling analysis through *CONTROL_IMPLICIT_BUCKLE. Analytical buckling loads are also obtained from the theoretical elasticity-based formulation shown in Ref. [10].

As shown in Fig. 5, both ABAQUS and ANSYS overpredict the buckling loads, but produce the same identical results as those from FEM B. Note that ABAQUS is based on the Jaumann rate of the Cauchy stress with constant moduli, as we identified in Sec. 3. Figure 6 shows the errors in predicting the buckling loads of Fig. 5. The relative errors are calculated with respect to the solutions from elasticity theory. The errors increase as the strip becomes thicker, i.e., as the significance of the orthotropic properties become more important.

Figure 7 shows the buckling load predictions from various FEA programs when the material properties vary. Figure 8 shows the relative errors in the computed buckling loads with respect to the analytical solutions. Again, the buckling loads predicted from FEM B, ABAQUS, and ANSYS are higher than those from the analytical solutions and other FEA programs. In the FEM B formulation with $m = 0$ and constant tangential moduli, an extra volumetric term enters in the total integration for the internal virtual work [4,10]. When the strip has strong orthotropic properties, the effects from this nonvanishing term become significant, as shown in Fig. 8, since the volumetric deformation is directionally dependent.

**4.2 Buckling Load Prediction for a Sandwich Structure With Orthotropic Constituents.** A sandwich beam or panel is a typical orthotropic structure that is widely used in practical engineering applications. Since finite element analysis is now commonly used to evaluate the mechanical performance of sandwich structures, commercial codes that are used to perform structural analysis containing orthotropic sandwich structures need careful examination. Figure 9 illustrates the loading and boundary configuration of the sandwich panel to be studied here. These are similar to the orthotropic strip studied before. Throughout the presentation, the superscript "*f*" represents quantities associated with the face sheets and "*c*" with the core. The face sheets and core are both orthotropic. The top and bottom face sheets are assumed to have the same geometric and material properties. The sandwich panel is subjected to a plane strain deformation in the *xy* plane. The FE model is created using quadrilateral plane strain elements. The results from an exact 2D elasticity solution [10,11], which serves as a benchmark, are used to evaluate the results obtained from the FE commercial codes.

Figure 10 compares buckling loads computed as a function of the stiffness ratio (between the longitudinal and transverse

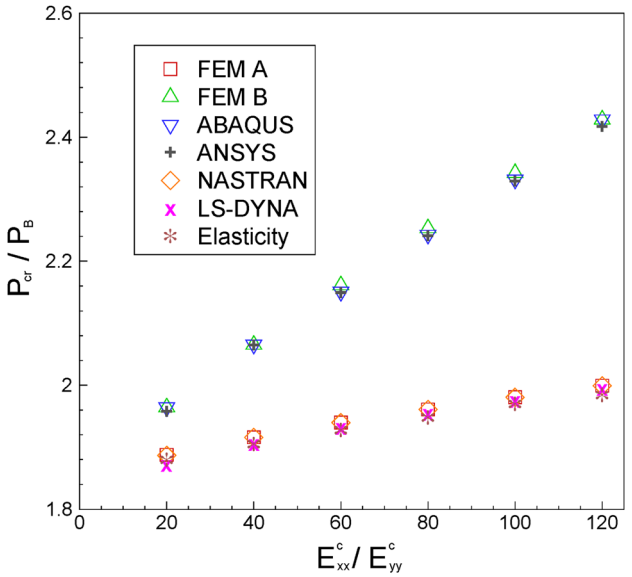


**Fig. 10 Comparison of the buckling load of a sandwich panel as a function of the stiffness ratio of the core between the transverse and longitudinal direction**

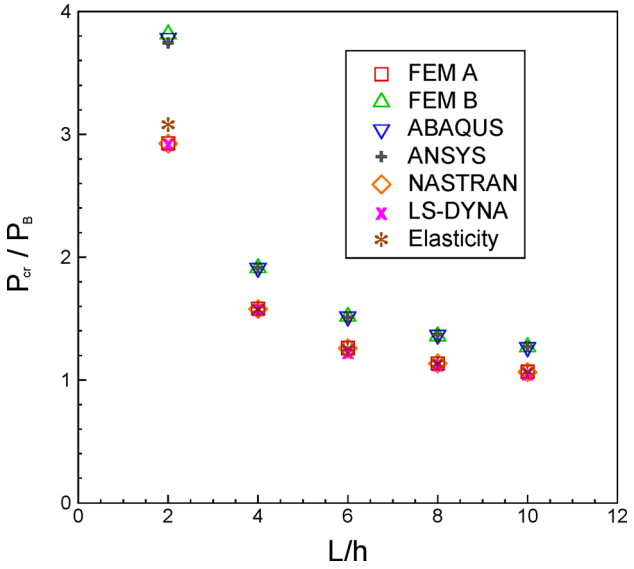


**Fig. 11 Comparison of the buckling load of a sandwich panel as a function of the panel aspect ratio**

**Table 3 Material properties of the face sheets and the core in Fig. 10**

| | Property | Value |
|---|---|---|
| | $E^f_{xx}$ (GPa) | 107 |
| | $E^f_{yy}$ (GPa) | 15 |
| Face sheet | $G^f_{xy}$ (GPa) | 4.3 |
| | $\nu^f_{xy}$ | 0.3 |
| | $h^f$ (mm) | 0.1 |
| | $E^c_{yy}$ (GPa) | $4 \times G^c_{xy}$ |
| Core | $G^c_{xy}$ (GPa) | $G^f_{xy}/200$ |
| | $\nu^c_{xy}$ | 0.25 |
| | $h^c$ (mm) | 0.8 |

**Table 4 Material properties of the face sheets and the core for the sandwich panel in Fig. 11**

| | Property | Value |
|---|---|---|
| | $E^f_{xx}$ (GPa) | 107 |
| | $E^f_{yy}$ (GPa) | 15 |
| Face sheet | $G^f_{xy}$ (GPa) | 4.3 |
| | $\nu^f_{xy}$ | 0.3 |
| | $h^f$ (mm) | 0.1 |
| | $E^c_{xx}$ (GPa) | $480 \times G^c_{xy}$ |
| | $E^c_{yy}$ (GPa) | $4 \times G^c_{xy}$ |
| Core | $G^c_{xy}$ (GPa) | $G^f_{xy}/200$ |
| | $\nu^c_{xy}$ | 0.25 |
| | $h^c$ (mm) | 0.8 |

direction) of the core. The material properties used for the results in Fig. 10 are listed in Table 3. The orthotropic material properties of the face sheets are obtained from Ref. [12]. The aspect ratio of the sandwich structure, $L/h$, is set to 3 for this example. Buckling loads in Fig. 10 are normalized by $P_B$ defined as

$$P_B = \frac{P_E}{1 + P_E/\overline{GA}} \tag{52}$$

where $P_E = 4\pi^2\overline{EI}/\mathrm{L}^2 =$ Euler's buckling load, $\overline{EI} =$ equivalent bending stiffness of a sandwich panel, and $\overline{GA} =$ equivalent shear resistance of a sandwich panel [13]. In Fig. 10, the buckling loads from FEM B, ABAQUS, and ANSYS are seen to be higher than the results from FEM A, NASTRAN, and LS-Dyna as the core stiffness ratio increases. The latter results agree with the exact 2D elasticity benchmark. It appears that, with increasing orthotropy of the core, the errors from the improper formulation (FEM B) become significant.

Figure 11 shows the buckling load comparison as a function of the aspect ratio (panel length to height ratio). Table 4 lists the material properties used in Fig. 11. FEM B, ABAQUS, and ANSYS again overpredict the buckling loads as the sandwich structure becomes thicker. As discussed earlier, the effect of the nonvanishing term, resulting from the incorrect formulation of the buckling problem, becomes significant when the core deformation is not negligible. Ji and Waas [10,11] have shown that, when the core has almost the same order of stiffness as the face sheets, predicted buckling loads from improper formulations result in large errors. One cannot simply neglect the axial load-carrying capacity of the core. Furthermore, when the constituents of a sandwich structure are orthotropic, the incorrect formulation is again seen to greatly overpredict buckling loads, even for sandwich panels with relatively soft cores, as shown in the examples here.

## 5 Conclusions

We have shown that neglecting to account for proper stress rates and work-conjugacy can lead to significant errors in finite element-based analysis when used for problems that require an incremental approach to obtaining a solution. By way of two examples, we have demonstrated that nonphysical solutions and incorrect critical loads are predicted by popular commercial codes that are now routinely adopted in structural analysis. We have shown that these codes can easily be fixed by abandoning the Jaumann rate of Cauchy stress and instead using the Truesdell rate with the correct, constant tangential moduli. Various types of stress rates and the corresponding internal work expressions have also been presented, and it is noted that most stress rates are paired with tangential moduli that are dependent on the current

stress. The internal work will be defined correctly only if proper tangential moduli are used when a specific type of stress rate is chosen. The choice among the different types of stress rates could be arbitrary, but the internal work should be defined properly, regardless of the choice. It is shown that buckling loads of thick orthotropic structures can be significantly overpredicted if the proper pairing for the internal work definition is not used. Various commercial FEA programs are examined here, and ABAQUS and ANSYS are identified as codes that adopt erroneous formulations based on the Jaumann rate of the Cauchy stress with constant tangential moduli. As shown here, this causes significant errors in the class of examples studied here. On the other hand, NASTRAN with the Marc solver and LS-DYNA have internal formulations that correctly predict the buckling loads of thick orthotropic structures; however, LS-DYNA predictions are inaccurate for the nonlinear incremental analysis related to the simple shear problem. NASTRAN, which is widely adopted for analyzing thin-wall structures, for which the significance of the errors that have been pointed out are not important, is seen to implement the correct FE formulation for both classes of problems that have been examined in this paper. We emphasize again that the switch to a fully work-conjugate formulation would be easy and this is highly recommended [4].

## Acknowledgment

We are grateful to Professor R. McMeeking, University of California, Santa Barbara, for thoughtful comments on an earlier version of the paper that led to improvement of our presentation.

## References

[1] Bazant, Z. P., 1971, "Correlation Study of Formulations of Incremental Deformation and Stability of Continuous Bodies," ASME J. Appl. Mech., **38**(4), pp. 919–928.
[2] Bazant, Z. P., and Cedolin, L., 1991, *Stability of Structures: Elastic, Inelastic, Fracture and Damage Theories*, Oxford University Press, New York.
[3] Hill, R., 1959, "Some Basic Principles in Mechanics of Solids Without Natural Time," J. Mech. Phys. Solids, **7**(3), pp. 209–225.
[4] Ji, W., Waas, A. M., and Bazant, Z. P., 2010, "Errors Caused by Non-Work-Conjugate Stress and Strain Measures and Necessary Corrections in Finite Element Programs," ASME J. Appl. Mech., **77**(4), p. 044504.
[5] Bazant, Z. P., Gattu, M., and Vorel, J., 2012, "Work Conjugacy Error in Commercial Finite Element Codes: Its Magnitude and How to Compensate for It," Proc. R. Soc. A, **468**(2146), pp. 3047–3058.
[6] Dienes, J. K., 1979, "On the Analysis of Rotation and Stress Rate in Deforming Bodies," Acta Mech., **32**(4), pp. 217–232.
[7] Lin, R., 2002, "Numerical Study of Consistency of Rate Constitutive Equations With Elasticity at Finite Deformation," Int. J. Numer. Methods Eng., **55**, pp. 1053–1077.
[8] Johnson, G. C., and Bammann, D. J., 1984, "A Discussion of Stress Rates in Finite Deformation Problems," Int. J. Solids Struct., **20**(8), pp. 725–737.
[9] Rivlin, R. S., 1948, "Large Elastic Deformations of Isotropic Materials. IV. Further Developments of the General Theory," Philos. Trans. R. Soc. London, Ser. A, **241**, pp. 379–397.
[10] Ji, W., and Waas, A. M., 2009, "2D Elastic Analysis of the Sandwich Panel Buckling Problem: Benchmark Solutions and Accurate Finite Element Formulations," Z. Angew. Math. Phys., **61**(5), pp. 897–917.
[11] Ji, W., and Waas, A. M., 2012, "Accurate Buckling Load Calculations of a Thick Orthotropic Sandwich Panel," Compos. Sci. Technol., **72**(10), pp. 1134–1139.
[12] Fagerberg, L., 2004, "Wrinkling and Compression Failure Transition in Sandwich Panels," J. Sandwich Struct. Mater., **6**(2), pp. 129–144.
[13] Bazant, Z. P., and Beghini, A., 2006, "Stability and Finite Strain of Homogenized Structures Soft in Shear: Sandwich or Fiber Composites and Layered Bodies," Int. J. Solids Struct., **43**(6), pp. 1571–1593.